European Polymer Journal 200 (2023) 112494

Contents lists available at ScienceDirect

European Polymer Journal

journal homepage: www.elsevier.com/locate/europolj

Sustainable antibacterial collagen composites with silver nanowires for resistive pressure sensor applications

Mireia Andonegi [a], Daniela M. Correia [b], Nelson Pereira [c], Margarida M. Fernandes [c,d], Carlos M. Costa [c,d,e], Senentxu Lanceros-Mendez [f,g,*], Koro de la Caba [a,f,*], Pedro Guerrero [a,f,h]

[a] BIOMAT Research Group, University of the Basque Country (UPV/EHU), Escuela de Ingeniería de Gipuzkoa, Plaza de Europa 1, 20018 Donostia-San Sebastián, Spain
[b] Center of Chemistry, University of Minho, 4710-057 Braga, Portugal
[c] Physics Centre of Minho and Porto Universities (CF-UM-UP), University of Minho, 4710-057 Braga, Portugal
[d] Institute of Science and Innovation for Bio-Sustainability (IB-S), University of Minho, 4710-053 Braga, Portugal
[e] Laboratory of Physics for Materials and Emergent Technologies, LapMET, University of Minho, 4710-057 Braga, Portugal
[f] BCMaterials, Basque Center for Materials, Applications and Nanostructures, UPV/EHU Science Park, 48940 Leioa, Spain
[g] Ikerbasque, Basque Foundation for Science, 48009 Bilbao, Spain
[h] Proteinmat Materials SL, Avenida de Tolosa 72, 20018 Donostia-San Sebastián, Spain

ARTICLE INFO

Keywords:
Collagen
Film
Sensors

ABSTRACT

Considering the circular economy and the increasing need of smart materials for the digitalization of society, it is essential that these materials are based on bio-resources. Thus, in order to replace synthetic by natural polymers in multifunctional composites, this work reports on the development of collagen/silver nanowires (Ag NWs) composites for resistive sensor applications. It is demonstrated the physical interactions of hydroxyl groups in collagen with the Ag NWs and that the Ag NWs are well dispersed within the collagen matrix. Further, the addition of Ag NWs to the collagen matrix increases the thermal stability of collagen and the Ag NW content does not affect the triple helix structure of the polymer matrix. The mechanical, electrical and antibacterial properties depend on Ag NW content and the best electric conductivity of 0.0515 S cm^{-1} is obtained for composites with 6 wt% of Ag NWs. This composite presents suitable resistance variations under pressure and bending allowing the development of sustainable multifunctional sensing composites with antibacterial activity that can be applied in next generation touch sensing electronic devices.

1. Introduction

Smart materials with different functionalities are being increasingly explored for different application areas, including sensors and actuators, biomedical, energy generation and storage, and environmental monitoring, among others [1,2]. The major advantage of these materials rely on their ability to react to changes in the surrounding microenvironment and provide a functional response [3–5]. The development of new smart materials with advanced functionalities has received a special attention in the last years, particularly the development of materials based on sustainable technologies [5], being the materials obtained from the combination of polymers with functional fillers (e.g. ionic liquids, nanoparticles or carbon nanotubes) among the most suitable for improving sustainability while maintaining high levels of functional performance [6–8]. Among all the available polymers, natural polymers derived from a wide variety of sources are gaining attention, being explored due to their high abundance in nature, which promotes the development of a new class of sustainable materials, processes and applications, and the reduction of fossil resources [9].

Biomaterials and, in particular, collagen based materials have become attractive candidates for a wide variety of functional applications because of their renewability, biocompatibility, biodegradability, availability and the possibilities for large-scale production. Collagen is the main component of a fibrous structural protein in connective tissues of vertebrates, being the building block of bones, tendons and skin, among others [10] and, therefore, valorization of wastes rich on collagen from food and leather industries can be a worthy approach to develop sustainable products [11,12]. Among all its properties, the high stretchability makes collagen a strong candidate for the development of sensoring devices, including bendable, conformable and wearable

* Corresponding author.
E-mail addresses: senentxu.lanceros@bcmaterials.net (S. Lanceros-Mendez), koro.delacaba@ehu.es (K. de la Caba).

https://doi.org/10.1016/j.eurpolymj.2023.112494
Received 14 June 2023; Received in revised form 15 September 2023; Accepted 9 October 2023
Available online 12 October 2023

sensors [8,13]. Concerning the electrical properties of this biomaterial, although the polar character of collagen provides interesting electrical properties, collagen electrical response is dominated by the stable dipole moments associated with water molecules [14]. Additionally, the chemical nature of collagen and its processing simplicity allows the combination with synthetic components to enhance specific properties and/or to develop sustainable composites with novel functionalities [15]. In this context, several studies have reported the use of carbon nanotubes and iron oxide nanoparticles as fillers in a collagen matrix in order to obtain electrically conductive biocomposites [16–18]. Further, collagen has been also combined with multi-walled carbon nanotubes (MWCNTs), allowing the development of composites with a strong potential to be applied as a real-time structural health monitoring, robotics and biomedical applications [19]. Further, collagen and collagen based composites have found applicability in smart health care systems, e-skin-based sensors and devices and implantable devices [20].

An interesting nanomaterial for the development of collagen based composites is silver, as it allows to combine excellent electrical properties with antibacterial activity, the latter being extremely relevant in the scope of antibiotic resistant bacteria in high traffic surfaces [21,22]. Further, collagen combined with silver nanoparticles has been also explored in the development of hydrogels for biomedical applications (wound infections treatment and wound healing) [20,23–25], electroactive biomimetic scaffolds, demonstrating excellent proliferation of embryonic cardiomyocytes [26], and on nonenzymatic amperometric biosensors of hydrogen peroxide [27].

Several studies have reported the combination of collagen with silver nanoparticles. However, silver nanowires display some interesting advantages comparing with the respective nanoparticles, such as their excellent electrical conductivity and improved optical properties at lower filler contents compared to nanoparticles [28].

Taking into account that the combination of collagen with silver nanowires is unexplored for multifunctional sensors, the goal of this work relies on the development of collagen composites with different amounts of silver nanowires (AgNW) with both resistive pressure sensing and also antibacterial activity. Collagen/AgNW nanocomposites were prepared by solvent casting technique by varying AgNW concentration. The morphological, thermal, mechanical, electrical and antibacterial properties were analyzed. The antibacterial studies have been performed both with gram-negative *Escherichia coli* and gram-positive *Staphylococcus aureus*. Finally, a proof of concept regarding the suitability of the developed materials as resistive sensor is presented.

2. Materials and methods

2.1. Materials

Collagen was supplied by Proteinmat materials S.L. (Spain). Silver nanowires (AgNWs), with diameter of 90–100 nm and length of 20–60 μm, were purchased by ACS Material and acetic acid by Panreac Quimica S.L.U (Barcelona, Spain).

2.2. Samples preparation

Collagen films with different Ag NW contents (0, 0.25, 0.5, 0.75, 1, 3 and 6 wt%) were prepared by solvent casting. Firstly, bovine skins were treated with NaOH 1 M at room temperature for 12 h and neutralized with phosphate buffer saline (PBS) solution in order to obtain native collagen, which was grinded and freeze-dried. Afterwards, collagen and the amount of Ag NWs required for each formulation were incorporated into 0.5 M acetic acid (1:40 collagen/acetic acid). The mixtures were stirred (150 rpm) at room temperature for 2 h, poured into Petri dishes, and left dry at room temperature to obtain the films. Films were designated as xAg, where × represents the corresponding Ag NWs content wt % in the samples. Films without Ag NWs were considered as control films. All films were conditioned in a climatic chamber (Alava Ingenieros, Spain) at 25 °C and 50 % relative humidity before testing.

2.3. Samples characterization

2.3.1. Physico-chemical characterization

Differential scanning calorimetry (DSC) analysis was carried out in a Mettler Toledo DSC 822. Samples (3.0 ± 0.2 mg) were sealed in aluminum pans to avoid mass loss during the experiment. Filled pans were heated from 25 to 300 °C at a rate of 10 °C/min under inert atmosphere conditions (10 mL N_2/min) to avoid thermo-oxidative reactions.

Fourier transform infrared (FTIR) spectra were obtained by using Alpha II Compact FTIR spectrometer equipped with attenuated total reflectance (ATR) crystal (ZnSe). A total of 32 scans were carried out at 4 cm^{-1} resolution. Data were recorded from 4000 to 800 cm^{-1}.

X ray diffraction (XRD) measurements were performed at 40 kV and 40 mA with a diffraction unit (PANalytical Xpert PRO, Madrid, Spain), generating the radiation from a Cu-Kα (λ = 1.5418 Å) source. Data were recorded from 2 to 50 °.

X-ray photoelectron spectroscopy (XPS) was performed in a SPECS spectrometer using a monochromatic radiation equipped with Al Kα (1486.6 eV). The binding energy was calibrated by Ag 3d5/2 peak at 368.28 eV. All spectra were recorded at 90° take-off angle. Survey spectra were recorded with 1.0 eV step and 40 eV analyser pass energy and the high-resolution regions with 0.1 eV step and 20 eV pass energy. All core level spectra were referenced to the C 1s neutral carbon peak at 284.6 eV. Spectra were analysed using the CasaXPS 2.3.19PR1.0 software, and peak areas were quantified with a Gaussian-Lorentzian fitting procedure.

For the scanning electron microscopy (SEM) measurements, films were placed on a metal stub and coated with gold using a JEOL fine-coat ion sputter JFC-1100 and argon atmosphere. Samples were observed using a Hitachi S-4800 scanning electron microscope (Hitachi, Madrid, Spain) at 15 kV accelerating voltage.

Bone-shaped samples (4.75 mm × 22.25 mm × 0.10 mm) were cut and an Instron 5967 mechanical testing system (Instron, Barcelona, Spain) was used to carry out tensile tests at 1 mm/min, according to ASTM D 638–03 standard.

Analysis of variance (ANOVA) was carried out with SPSS software (SPSS Statistic 25) to determine significant differences between samples. Tukey's test with a statistically significance at the $P < 0.05$ level was considered for multiple comparisons among different systems.

The electrical conductivity (σ) of the collagen/Ag NW composites was carried out through a Keithley 287 picoammeter/voltage source with an applied voltage between ± 10 V at room temperature using a parallel plate configuration. Before measurements, gold electrodes of 5 mm diameter were sputtered on each side of the sample, parallel to each other, with a Polaron SC502 apparatus.

The electrical conductivity (σ) value was calculated through equation (1):

$$\sigma = \frac{d}{R.A} \tag{1}$$

where R is the composite resistance, obtained from the slope of the I-V curves, A is the area, and d is the sample thickness.

2.3.2. Antibacterial studies

Gram-negative *Escherichia coli* ATCC® 8739™ and gram-positive *Staphylococcus aureus* ATCC® 6538™ were purchased from American Type Culture Collection (LGC Standards S.L.U, Spain). The bacterial preinoculum was prepared from a single colony of the corresponding stock bacterial culture, which was resuspended in nutrient broth (NB) and then incubated overnight at 37 °C, and 110 rpm. After 20 h, the bacteria were harvested by centrifugation at 4500 rpm for 5 min and resuspended in NaCl 0.9 % (w/v) twice. The *E. coli* cultures optical density

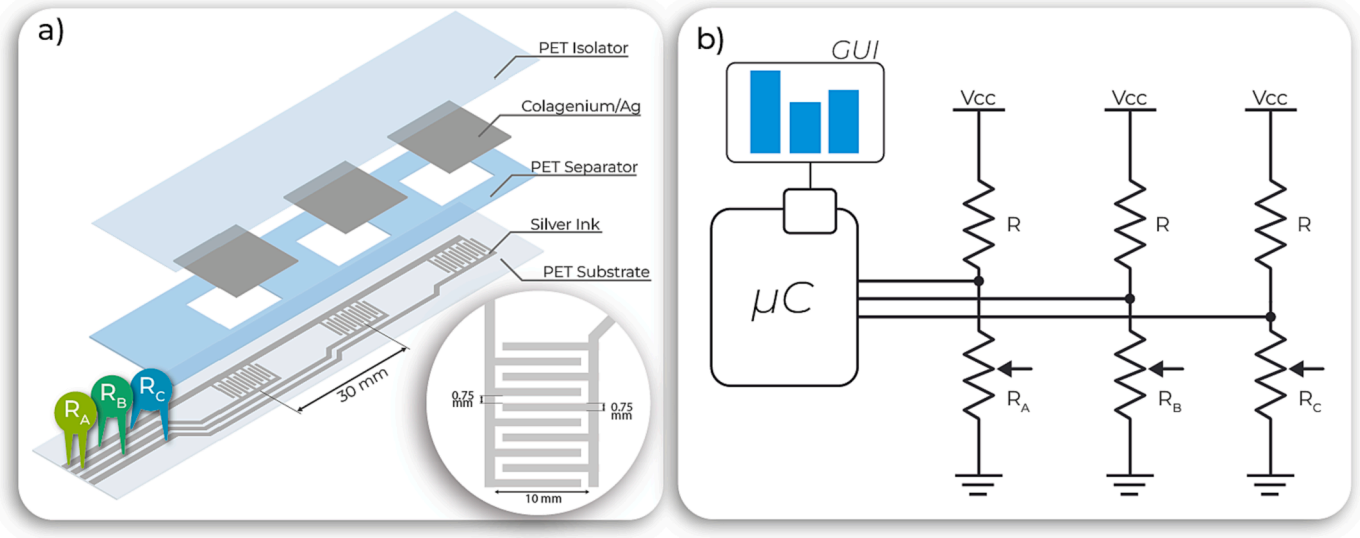

Fig. 1. A) assembly process of the pressure sensitive collagen/ag nw film sensors and b) schematic representation of the electronic circuit for data acquisition.

(OD) was adjusted to OD = 0.26 and the *S. aureus* cultures OD was adjusted to 0.2 with NaCl 0.9 % (w/v) measured at 600 nm, giving rise to a working inoculum of approximately 1×10^8 colony forming units (CFU) per mL.

2.3.2.1. Colony forming units. The bactericidal activity was assessed according to the standard shake flask method (ASTM-E2149-01) with some modifications. This method provides quantitative data for measuring the reduction rate in number of bacteria colonies formed, converted to the average colony forming units per millilitre of buffer solution in the flask (CFU/mL). To evaluate the potential of the materials with embedded increasing concentration of Ag NW, to eradicate *E. coli* and *S. aureus*, samples with 1 cm × 1 cm in size, previously sterilized under UV light for 30 min each side, were placed in contact with each bacterial inoculum (1 mL of working inoculum) in 15 mL falcon tubes. The tubes were then placed under vigorous agitation (220 rpm) at 37 °C for 2 h. The bacterial solution in contact with the material and respective controls were then removed and the surviving colonies were quantified by serially diluting (1:10) in sterile buffer solution, plated on a plate count NB agar and further incubated at 37 °C for 24 h. Antimicrobial activity is reported in terms of bacteria log reduction calculated as the ratio between the number of surviving bacteria after and before the contact with the materials according to equation (2).

$$Bacteriallog_{10}reduction(\%) = log_{10}(A) - log_{10}(B) \quad (2)$$

where A and B are the average number of bacteria before and after the contact with the samples, respectively. The results were further expressed as $\log_{10}$ reduction by calculating the $\log_{10}$ of bacteria reduction. All antibacterial data represent mean values of 3 independent assays ± SD (n = 3).

2.3.3. Sensor device development

For the development of the pressure sensors, in a first step the nanoparticle silver ink from Novacentrix (Metalon HPS-021L) was manual screen printed on top of a PET substrate using a screen of 100 threads by cm, creating an array of three conductive interdigits. Then, a PET film separator with 100 μm of thickness with three holes (10 mm × 12 mm) was glued to the interdigitated PET substrate using double sided tape (3 M, RP45F VHB). Composite collagen films with an area of 12 mm × 14 mm and a thickness of ~ 100 μm were glued with double sided tape to another PET film separated by 30 mm (to be on top of the interdigits). The composite films on the PET substrates were glued on top of the PET separator allowing the collagen/Ag NW films to touch the conductive interdigits when a pressure was applied (Fig. 1) due to an air gap. The chosen configuration with interdigits and an air gap between the collagen film and printed silver fingers enables the detection of pressure without relying on the internal resistance variation of the collagen film (piezoresitive effect), instead of utilizing the area of contact between the collagen film and the fingers where the pressure sensing mechanism works on the same principle as commercially available FSR (force sensing resistor) sensors that change the resistive value based on the degree of pressure.

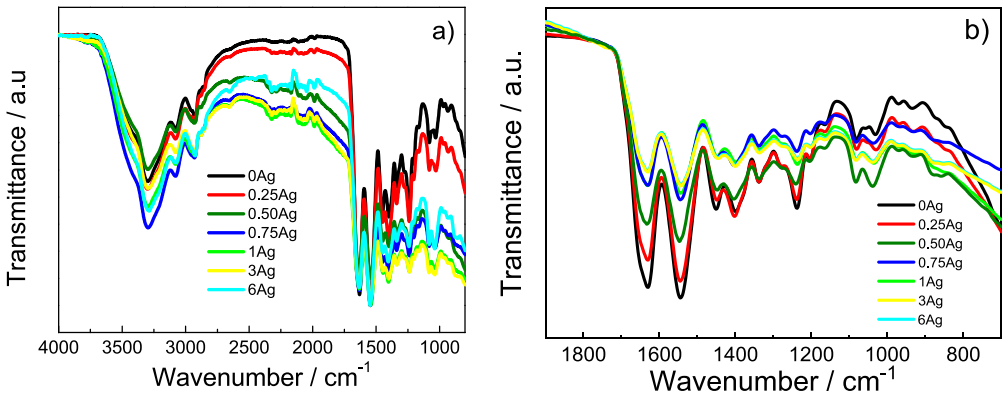

Fig. 2. FTIR spectra of collagen films with different contents of Ag NWs: a) from 4000 to 800 cm^{-1} and b) from 1800 to 800 cm^{-1}.

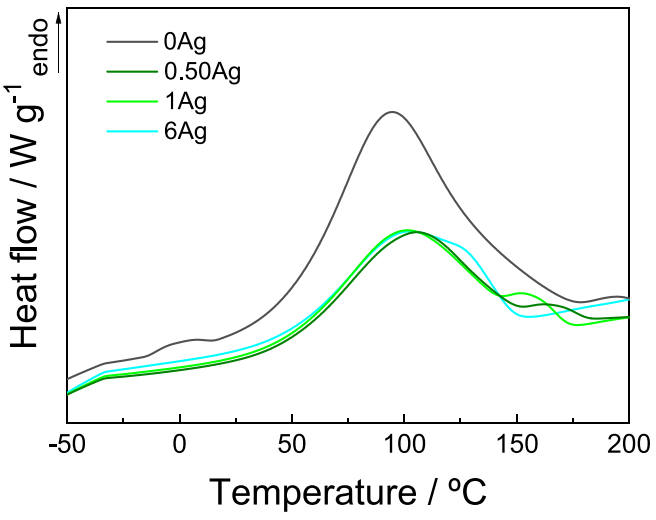

Fig. 3. DSC curves of collagen films with different contents of AgNWs.

Table 1
Glass transition temperature (T_g), denaturation temperature (T_d), and enthalpy (ΔH) of the collagen samples obtained by DSC analysis.

	$T_g \pm 1$	$T_d \pm 1$	ΔH ± 1 (mJ/g)
	(°C)	(°C)	
0Ag	46.9	94.2	275.7
0.25Ag	49.2	100.4	157.8
0.50Ag	50.9	102.4	138.0
0.75Ag	50.9	103.8	137.9
1Ag	51.2	103.9	137.2
3Ag	51.3	104.2	136.8
6Ag	51.4	105.1	136.6

The pressure sensors were connected to a microcontroller board, Teensy 4.0 from PJRC, for interfacing with a graphical user interface (GUI) built on python. An electronic circuit composed by 3 voltage dividers were connected to the 12 bits analog-to-digital converter integrated with the microcontroller, and the collected data were sent directly to the GUI application via universal serial bus (USB).

3. Results and discussion

3.1. Physicochemical and thermal properties

The interactions among the components of the films and the effect of the Ag NWs in the collagen structure were evaluated by FTIR analysis. As represented in Fig. 2, all samples show the characteristic absorption bands of collagen: amide A (N–H and O–H stretching), amide I (C = O stretching), amide II (N–H bending), and amide III (C-N stretching) at 3300, 1630, 1542 and 1240 cm^{-1}, respectively [29,30]. The broad band at 3300 cm^{-1} is also attributed to the OH stretching of the hydrogen-bonded network formed by water molecules around collagen [31]. Additionally, the hydroxyl group in collagen has strong affinity to silver ions and, therefore, physical interactions, such as van der Waals forces, may be present among the hydroxyl groups of collagen and the positive charge of silver [32,33]. Overall, the absorption bands in the spectra of all samples are relatively similar to those of the control films, independently of the filler content.

The effect of the inclusion of Ag NWs on the thermal stability of collagen was assessed by DSC analysis (Fig. 3). All samples showed an endothermic peak between 35 °C and 175 °C, resulting from dehydration and thermal denaturation of the collagen amorphous region [34].

The temperature values of glass transition (T_g) and thermal denaturation (T_d) of collagen and the corresponding Ag NW composites are shown in Table 1. It is observed that T_g and T_d increase from 46.9 °C and 94.2 °C to 49.2 °C and 100.4 °C, respectively, when 0.25 wt% Ag NWs are added. When higher contents of Ag NWs are added up to 6 wt% filler content, T_g and T_d values slightly increase further up to 51.39 °C and 105.14 °C, respectively. These demonstrate that the addition of Ag NWs enhances the thermal stability of collagen, probably due to the changes in collagen morphological and structural variations observed by SEM (Fig. 3), XRD (Fig. 4) and XPS (Fig. 5) analyses. The decrease in the free water content of the films observed by FTIR analysis also contributes to the increase of both transition temperatures [35]. Furthermore, the enthalpy (ΔH) value, which represents not only the collagen denaturation when structural water is released, but also the energy required to release free and bound water [36], decreases sharply from 275.7 mJ/g to 157.8 mJ/g when 0.25 wt% Ag NWs are added and slightly when higher content of Ag NWs are further included in the composite. These results are in agreement with the decrease of the free and bound water content with the addition of Ag NWs [37,38], as observed by FTIR analysis (Fig. 1).

3.2. Morphological and structural characteristics

SEM, XRD and XPS analyses were carried out in order to determine the variations in the microstructure and structure of the samples after filler addition. Concerning the SEM images (Fig. 4), the cross-section of all samples show the fibrillar structure typical of collagen [39,40], while the surface images show the suitable Ag NWs dispersion in the collagen matrix. Just small Ag NWs agglomerates are observed in the composite samples, which are well distributed and independent of the filler content.

Regarding XRD analysis (Fig. 5), all samples show the characteristic amorphous structure of collagen, with a broad peak around 20 °, associated with the diffuse scattering of collagen fibers, and the peak at 7 ° that represents the triple helix structure of collagen [41,42]. As observed in Fig. 5a, the structural order of collagen increases when Ag NWs are incorporated, since an increase in the intensity of the peak at 7 ° is observed for filler concentrations up to 1 wt% Ag NWs. This increase is attributed to the C-O interactions between the carboxylic groups of the amino acids and the Ag NWs, whose low frequency vibrations cannot be detected by FTIR spectroscopy [43], as well as due to the van der Waals interactions between silver and hydroxyl groups in collagen, as suggested by FTIR analysis. Nevertheless, the incorporation of higher contents of Ag NWs leads to a decrease of the structural order of collagen with respect to those samples with Ag NWs contents lower than 1 wt%, attributed to the fact that large filler content typically represents defective structures hindering structural order formation, opposite to low filler contents that allow to nucleate order formation [44].

Additionally, the XRD spectra from 2 to 50 ° is shown in Fig. 5b. The peaks at 38.4 ° and 44.8 ° are assigned to the diffraction of (1 1 1) and (2 0 0) planes of silver [45,46], and the peaks at 28 ° and 32.5 ° are related to AgCl impurities and correspond to (1 1 1) and (2 0 0) planes [40], respectively.

XPS was performed to get a detailed insight into the corresponding elemental composition of the samples (Fig. 6a). The peak of O 1s at 531.9 eV is attributed to O-C=O and O=C-N, while the peak of N 1s at 399.7 eV is attributed to C = N and C-N. The deconvolution of the experimental C 1s spectrum results in three peaks (Fig. 6b): the peak at 284.6 eV is assigned to the aliphatic carbons (C–H/C–C), the peak at 285.9 eV is attributed to the carbons associated with oxygen or nitrogen (C-O/C-N), and the peak at 288.1 eV is related to carbons in the peptidic chains in collagen (C = O/N-C = O) [47]. The relative area of these three peaks changes when Ag NWs are added, as shown by the representative results for 1Ag presented in Fig. 6c. Specifically, the relative area of the peak at 284.6 eV (C–H/C–C) slightly decreases, indicating that the hydrophobic character decreases, while the relative area of the peaks at 284.6 (C-O/C-N) and 287.8 eV (C = O/N-C = O) increases, suggesting the orientation of polar groups towards the outer layers, in agreement

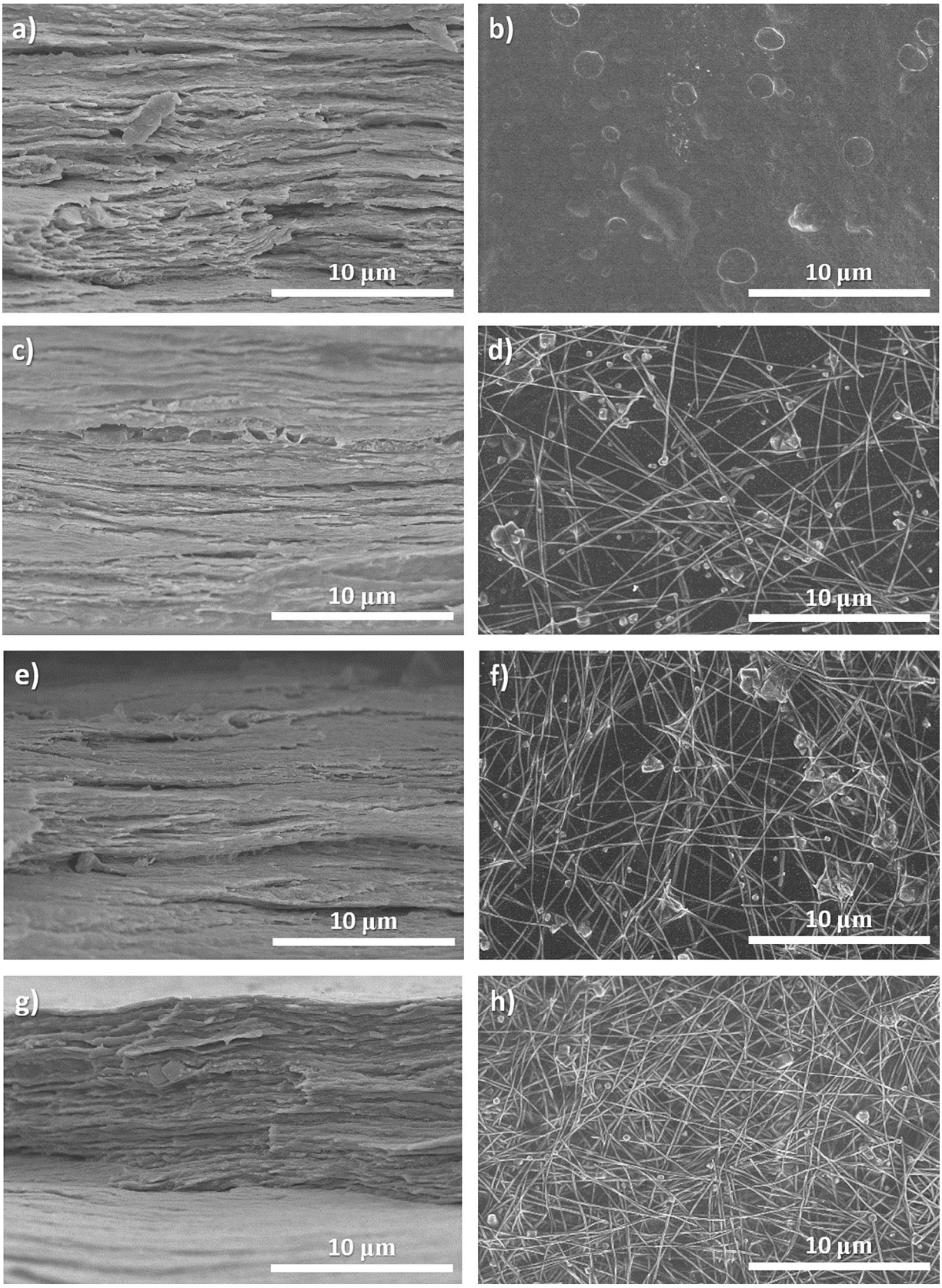

Fig. 4. Representative cross-section SEM images of a) 0Ag, c) 0.5Ag, e) 1Ag and g) 3Ag samples; surface images for b) 0Ag, d) 0.5Ag, f) 1Ag and h) 3Ag.

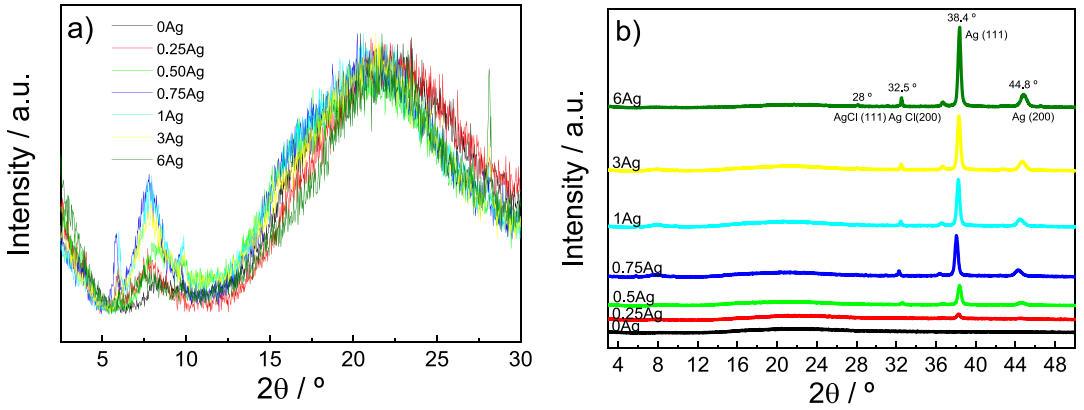

Fig. 5. XRD pattern of the pristine collagen and composite samples with Ag NW: a) from 2.5 ° to 30 ° and b) from 2.5 ° to 50 °.

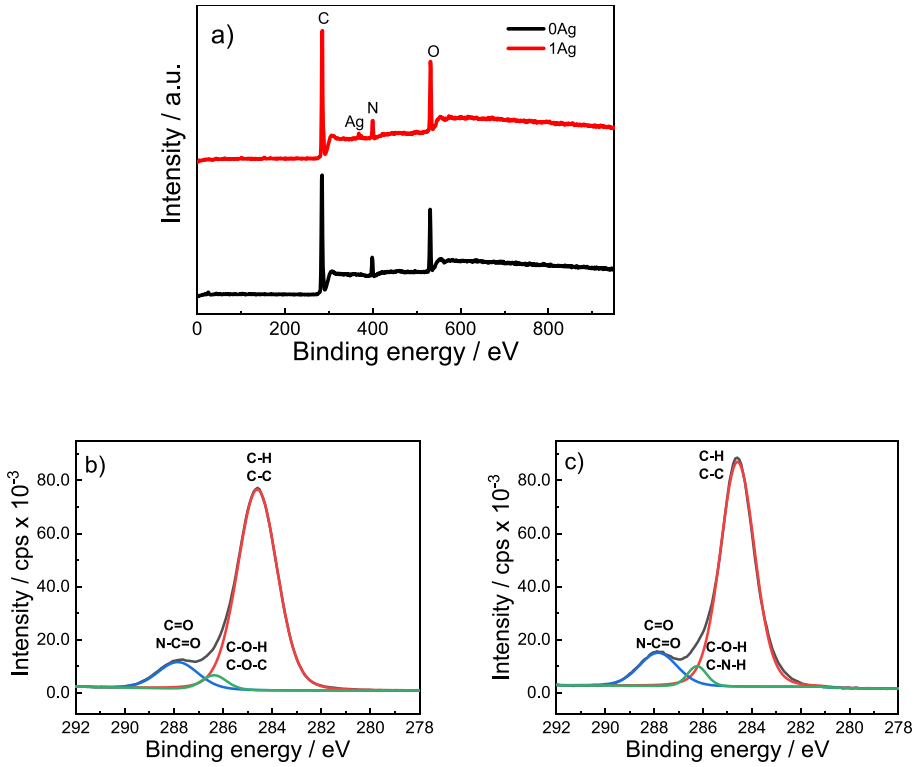

Fig. 6. XPS spectra of a) pristine collagen (0Ag) and 1Ag samples and XPS spectra and deconvolution curves for C 1 s features for the b) pristine (0Ag) sample and c) 1Ag sample.

Table 2
Area of the XPS spectra peaks for collagen and 1Ag composite samples.

Area (%)	C–C/ C–H 284.6 (eV)	C-O/ C-N 286.2 (eV)	C = O/ N-C = O 287.8 (eV)	C = N/ C-N 399.7 (eV)	O-C = O/ O = C-N 531.3 (eV)	Ag (3d5/2) 368.1 (eV)
0Ag	69.5	3.1	9.3	5.9	12.2	0
1Ag	66.6	3.4	10.8	5.5	13.6	0.1

with the decrease of hydrophobicity.

For a better understanding of the changes of the samples, the areas under the curves were calculated. As presented in Table 2, there are no relevant differences between the relative areas with the addition of Ag NWs, indicanting the abscense of covalent reactions. A weak peak with a relative area of 0.1 % was observed at 368.1 eV in 1Ag sample. This peak is related to Ag (3d5/2) and is in good agreement with previously reported values, indicating that the chemical state of nanowires consists mainly of metallic silver instead of silver oxide [48,49]. The lack of great alterations of the chemical groups with the addition of Ag NWs is indicative of the chemical stability of the system, a desirable property for the intended film application.

3.3. Mechanical properties

Tensile tests were performed in order to evaluate the effect of the filler content and the corresponding variations on the mechanical properties of collagen samples. As can be seen in Fig. 7, the fibres of collagen were orientated as the elongation increased, increasing tensile resistance up to the point of break.

The results of the elastic modulus (EM), tensile strength (TS) and

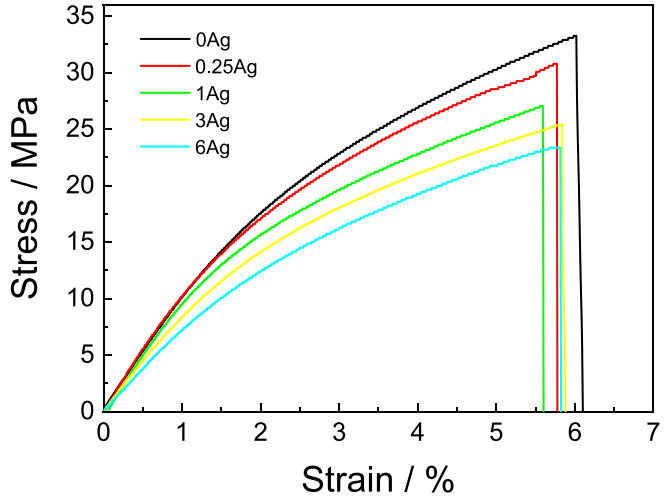

Fig. 7. Stress–strain curve of 0Ag, 0.25Ag, 1Ag, 3Ag and 6Ag samples.

Table 3
Elastic modulus (EM), tensile strength (TS) and elongation at break (EB) of collagen films prepared with different Ag NWs contents.

Films	EM (MPa)	TS (MPa)	EB (%)
0Ag	1334 ± 86[a]	33.21 ± 2.42[a]	6.01 ± 0.28[a]
0.25Ag	1333 ± 93[a]	31.62 ± 2.01[a]	5.76 ± 0.42[a]
0.5Ag	1235 ± 65[a]	30.55 ± 0.64[a,b]	5.86 ± 0.34[a]
0.75Ag	1062 ± 83[b]	28.09 ± 2.04[b]	5.81 ± 0.51[a]
1Ag	991 ± 54[b]	26.87 ± 2.30[b]	5.60 ± 0.42[a]
3Ag	818 ± 32[c]	24.98 ± 2.34[c]	5.75 ± 0.29[a]
6Ag	712 ± 28[c]	22.60 ± 2.22[c]	5.87 ± 0.31[a]

[a-c] Two means followed by the same letter in the same column are not significantly ($P > 0.05$) different through the Tukey's multiple range test.

elongation at break (EB) are shown in Table 3. It is observed that EM and TS values slightly decreased ($P < 0.05$) when Ag NWs are incorporated into collagen formulations. These results are in good agreement with other works in which silver nanoparticles are added into biopolymers, such as gelatin, agar and starch [50–52]. These results can be attributed to the reduction of interlinking density, as the mechanical properties of composite films depend on the interactions between components and their miscibility, as well as on the interactions between polymer chains [32]. Concerning EB values, no significant differences are observed with the addition of Ag NWs.

3.4. Electrical properties

The D.C. electrical conductivity of the collagen/Ag NW composites has been obtained through the I-V curves represented in Fig. 8a). It is observed that the slope of the I-V curves increases with increasing Ag NW content indicating that the incorporation of conductive silver nanowires into the collagen matrix promotes an increase in electrical conductivity of the samples.

The electrical conductivity was determined from the I-V curves and equation (1), Fig. 8b representing the electrical conductivity value as a function of Ag NW content for collagen and the corresponding Ag NW composites.

It is observed that the D.C. electrical conductivity (σ) increases with increasing filler content in the composites. For 0.25 wt% of Ag NW, the σ value increases in two orders of magnitude with respect to pristine collagen. The percolation threshold [53] is between 0.25 and 0.5 wt% and the maximum electrical conductivity value of 0.0515 S cm^{-1} is obtained for the sample with 6 wt% Ag NW content. This behavior is attributed to the formation of an electrically conductive network in the collagen/Ag NW composite with increasing filler content, as described by the percolation theory [53].

3.5. Antibacterial properties

The pristine collagen and composite materials with increasing concentration of silver nanowires were tested against two representative pathogens, one gram-positive, *S. aureus,* and one gram-negative, *E. coli.* The material was placed in contact with saline solution containing bacteria for 2 h and the amount of bacteria in the medium (planktonic) was quantified. It is observed that collagen does not possess antibacterial activity, and that this activity increases with increasing filler

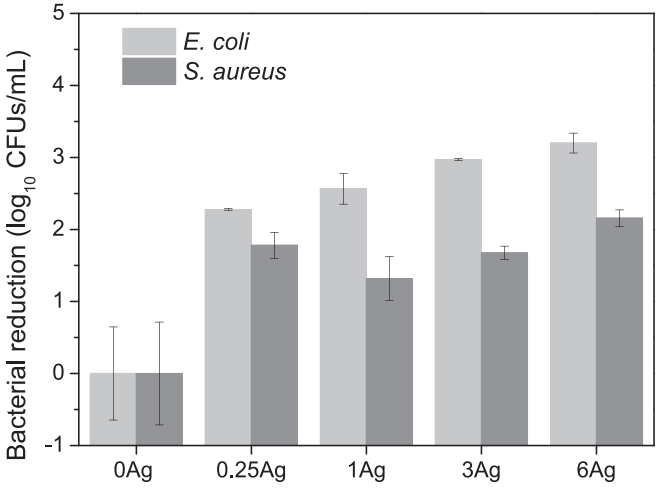

Fig. 9. Antimicrobial activity of silver-containing materials against *E. coli* and *S. aureus*, measured in $\log_{10}$ reduction of CFUs.

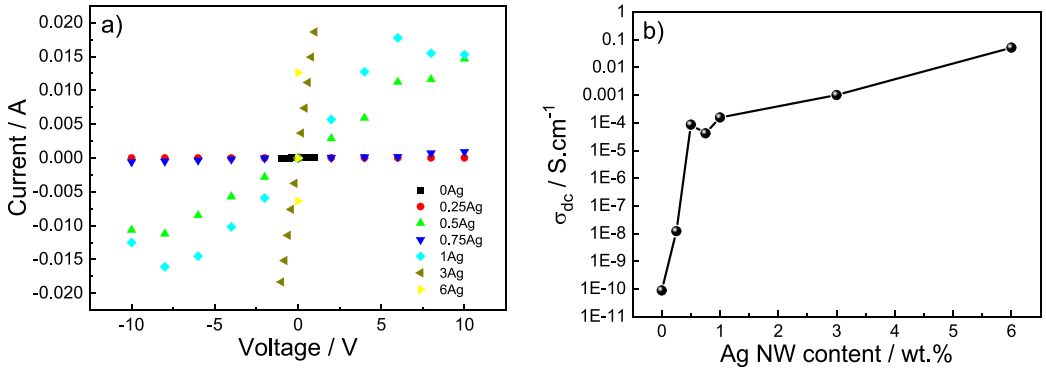

Fig. 8. A) current-voltage (*I-V*) curves for collagen/Ag NW composites and b) electrical conductivity of the nanocomposites as a function of Ag NW content.

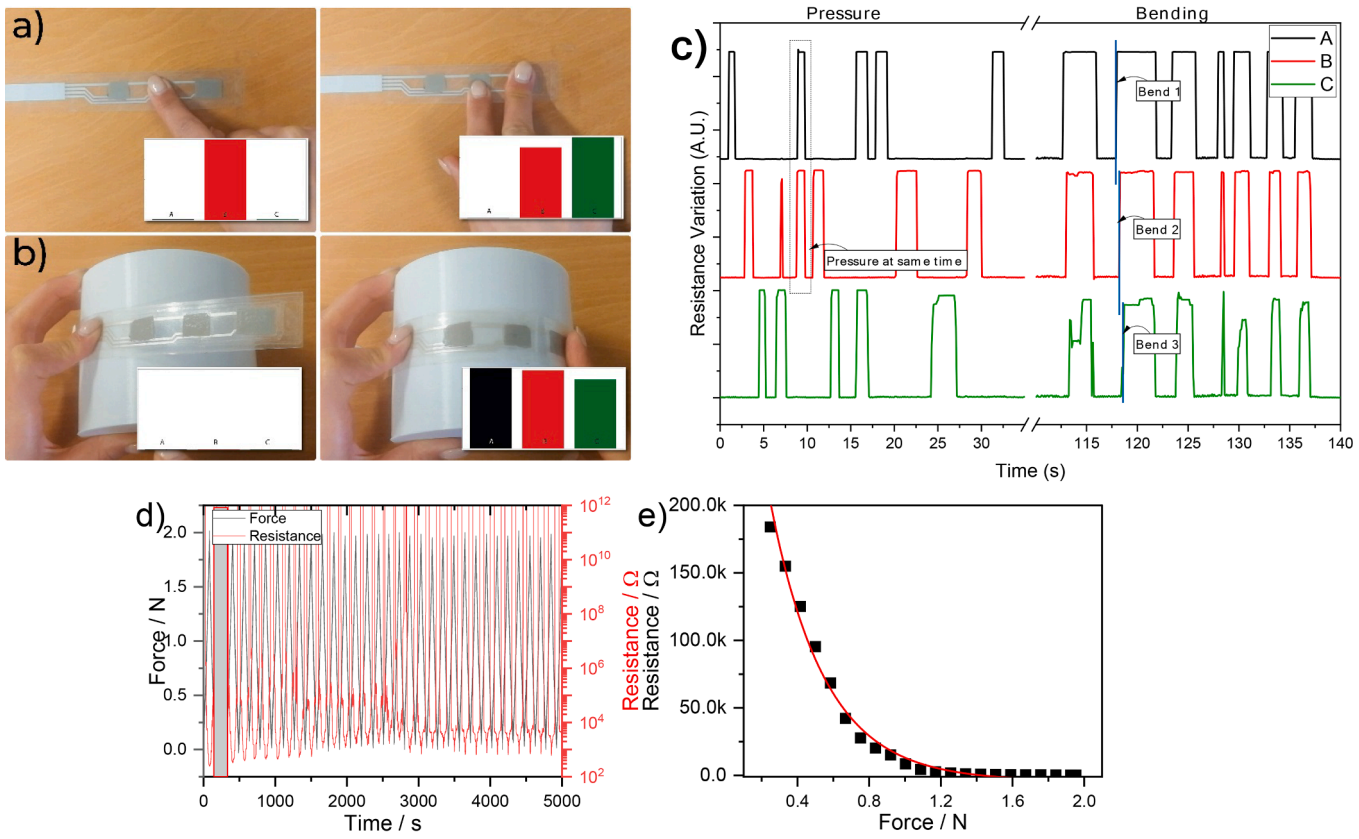

Fig. 10. Resistance variation of the 3 pressure sensors. a) Pressure event directly on top of the sensors. b) Bending of the sensors on top of a cylinder. c) Corresponding resistance variation as a function of time (see also supplementary video). d) Resistance variation as a function of the force applied to the sensor. e) Sensitivity of the sensor.

concentration (Fig. 9).

After incorporating silver, both bacteria were inactivated in a concentration dependent manner. In the case of *S. aureus*, a 2 $\log_{10}$ reduction was obtained with 6 wt% of silver (6Ag) composite, which means a 100-fold reduction (99 %) in bacteria. For *E. coli*, results show a larger effect, being reduced in 3 $\log_{10}$, meaning that there was 1000-fold less bacteria in the medium.

The inherent morphology of the gram-positive bacteria, comprising a thick layer of a peptidoglycan layer [54], may hinder the action of silver ions through the membrane of *S. aureus* when compared to the gram-negative cell wall, as previously reported [22,55]. In fact, silver-based materials have been reported to be more effective in hydrated and nutrient-poor environments, such as the ones used in this study. This is due to the fact that silver ions often react with thiol groups from proteins and components in the medium [56]. Since the antimicrobial studies have been performed in saline solution rather than in nutrient-rich medium, it is reasonable to assume that silver does not face competing reactions in the medium, thus being more active towards the bacteria. This is beneficial when the materials are to be applied in environments where hydration is often present such as kitchens or bathrooms.

3.6. Sensor response

Taking into account that the collagen composite with the high electrical properties and antibacterial activity was the composite with 6 wt% of Ag NW, it was used for the development of a resistive sensor. The sensor response is shown in Fig. 10 and in the supplementary video (see supplementary information).

Fig. 10a and b) show a visual image and the results of the resistance variation of the 3 sensors when two different events occur: pressure and bending events, respectively. Fig. 10c represents the corresponding resistance variation as a function of time for the pressure and bending events shown in Fig. 10a and b. In Fig. 10a, a finger pressure was applied directly on top of the sensors and in Fig. 10b, a bending movement is applied on a cylinder-shaped object. In both events, the sensor allows the identification of the pressure and bending variation on multiple sensors at the same time for mechanical tactile buttons and when the sensors array is bent. In both cases, the observed response is attributed to the reduction of the air gap between the interdigit and the collagen/Ag NW composites, allowing to detect a bending motion that can be also used in touch and finger flexing detection in robotic applications, among others.

In order to access the relationship between the resistance variation and the applied force, the sensor was placed on a Shimadzu autograph AG-IS, with a load cell of 500 N. Compression cycles ranging from 0 to 2 N were conducted at a constant rate of 1 mm/min, as shown in Fig. 10d). The designed sensor presents the best detection from 0.4 to 1.4 N, starting to saturate for higher forces. Forces lower than 0.4 N cannot be detected by the sensor. The variation of the resistance of the sensor can be described by nonlinear behavior, as shown in Fig. 10e).

Considering the current emphasis on sustainability and environmentally-friendly materials, the proposed sensor offers a reduced environmental footprint compared to the recently reported pressure sensing materials [57]. Most of these materials rely on a combination of synthetic matrices such as perfluoroalkoxy alkane (PFA) [58], polyimide (PI) [59], and polyvinylidene difluoride (PVDF) [60], along with fillers like carbon nanotubes (CNTs) [61], metal nanowires [62], and metal nanoparticles (NPs) [63], while this work proposes a more sustainable alternative by substituting a synthetic matrix with a biopolymer. In this context, even though there have been studies exploring the use of collagen for pressure sensing applications, the chemicals employed in processing these composites can be highly

detrimental to the environment [64–66]. For instance, Ma et al. [64] developed high-sensitivity microchannel-structured collagen fiber-based sensors, utilizing glutaraldehyde as a crosslinking agent and HCl as a solvent, both of which have significant environmental pollution potential.

4. Conclusions

Collagen composites with silver nanowires (Ag NW) have been developed by solvent casting with varying Ag NW content from 0 to 6 wt %. The addition of the nanofillers allows to improve the thermal stability of the collagen polymer, the behaviour being independent of the Ag NW content. Independently of the filler content, a good dispersion of the filler was observed, being the samples mechanically stable. A maximum of electrical conductivity of 0.0515 S cm^{-1} has been obtained for the sample with 6 wt% filler content. With respect to the functional response, a filler dependent antibacterial activity has been obtained for both gram-positive and gram-negative bacteria. A proof of concept regarding the potential applicability of the developed materials as a resistive sensor has been demonstrated, being the materials able to detect both pressure and bending events with excellent behavior. Thus, this work demonstrates the potential development of sustainable multifunctional composites with antimicrobial properties for electronic devices based on bio-based resources suitable for sensor applications.

CRediT authorship contribution statement

Mireia Andonegi: Data curation, Formal analysis, Methodology, Investigation, Writing – original draft. **Daniela M. Correia:** Data curation, Formal analysis, Methodology, Investigation, Writing – original draft. **Nelson Pereira:** Data curation, Formal analysis, Investigation, Writing – original draft. **Margarida M. Fernandes:** Methodology, Investigation, Writing – original draft. **Carlos M. Costa:** Conceptualization, Methodology, Investigation, Resources, Supervision, Validation, Writing – review & editing. **Senentxu Lanceros-Mendez:** Conceptualization, Investigation, Resources, Funding acquisition, Project administration, Supervision, Validation, Writing – review & editing. **Koro de la Caba:** Investigation, Resources, Funding acquisition, Project administration, Supervision, Writing – review & editing. **Pedro Guerrero:** Conceptualization, Methodology, Supervision, Writing – review & editing.

Declaration of Competing Interest

The authors declare that they have no known competing financial interests or personal relationships that could have appeared to influence the work reported in this paper.

Data availability

Data will be made available on request.

Acknowledgments

Grant PID2021-124294OB-C22 funded by MCI/AEI10.13039/501100011033 and by “ERDF A way of making Europe”. This work was also supported by the Basque Government (IT1658-22) and the Portuguese Foundation for Science and Technology (FCT) under strategic funding UIDB/04650/2020, UID/FIS/04650/2021, project PTDC/FIS-MAC/28157/2017, and Investigator FCT Contract 2020.02915.CEECIND (D.M.C) and 2020.04028.CEECIND (C.M.C.) and grant SFRH/BPD/121464/2016 (M.M.F), funded by national funds through FCT and by the ERDF through the COMPETE2020-Programa Operacional Competitividade e Internacionalização (POCI). The authors also acknowledge funding from the Basque Government Industry and Education Department under the ELKARTEK program. M.A. thanks the Basque Government for her fellowship (POS_2022_1_0007).

Appendix A. Supplementary material

Supplementary data to this article can be found online at https://doi.org/10.1016/j.eurpolymj.2023.112494.

References

[1] A. Bhatnagar, S. Wagh, B. Singh, R.R. Agarwal, F. Khan, Smart materials – a review, Annals of Dental Specialty. 4 (2016) 10–12.
[2] W.G. Drossel, H. Kunze, A. Bucht, L. Weisheit, K. Pagel, Smart3 – smart materials for smart applications, Procedia CIRP. 36 (2015) 211–216.
[3] H.C. Kim, S. Mun, H.U. Ko, L. Zhai, A. Kafy, J. Kim, Renewable smart materials, Smart Mater. Struct. 25 (2016).
[4] P.D. Mangalgiri, Challenges in modeling of smart materials and devices. International Workshop on Smart Devices - Modeling of Material Systems. Chennai, INDIA2008. p. 13-+.
[5] A. Mishra, A. Gangele, Smart Materials For Clean And Sustainable Technology For Smart Cities. National Conference on Smart Materials - Energy and Environment for Smart Cities (NSES). SI ed. Gwalior, INDIA2018. p. 338-42.
[6] I. Kang, J.Y. Jung, G.R. Choi, H. Park, J.W. Lee, K.J. Yoon, Y. Yeo-Heung, V. Shanov, M.J. Schulz, Developing carbon nanocomposite smart materials. 7th International Symposium on Nanocomposites and Nanoporous Materials (ISNAM7). Gyeongju, SOUTH KOREA2006. p. 207-+.
[7] B. Araldi da Silva, R. de Sousa Cunha, A. Valério, A. De Noni Junior, D. Hotza, S.Y. Gómez González, Electrospinning of cellulose using ionic liquids: An overview on processing and applications, Eur. Polym. J.. 147 (2021) 110283.
[8] Z. Peng, S. Zheng, X. Zhang, J. Yang, S. Wu, D. Ding, L. Lei, L. Chen, G. Feng, Flexible wearable pressure sensor based on collagen fiber material, Micromachines (Basel) (2022) 13.
[9] A.C.Q. Silva, A.J.D. Silvestre, C. Vilela, C.S.R. Freire, Natural polymers-based materials: a contribution to a greener future. 27,94, 2022.
[10] J.-Y. Exposito, U. Valcourt, C. Cluzel, C. Lethias, The fibrillar collagen family, Int. J. Mol. Sci. 11 (2010) 407–426.
[11] K.L. Ong, G. Kaur, N. Pensupa, K. Uisan, C.S.K. Lin, Trends in food waste valorization for the production of chemicals, materials and fuels: case study South and Southeast Asia, Bioresour. Technol. 248 (2018) 100–112.
[12] P. Thanikaivelan, J.R. Rao, B.U. Nair, T. Ramasami, Recent trends in leather making: processes, problems, and pathways, Crit. Rev. Environ. Sci. Technol. 35 (2005) 37–79.
[13] H. Pan, T.-W. Lee, Recent progress in development of wearable pressure sensors derived from biological materials (2021) 10,2100460.
[14] M. Ashoorirad, M. Saviz, A. Fallah, On the electrical properties of collagen macromolecule solutions: role of collagen-water interactions, J. Mol. Liq. 300 (2020), 112344.
[15] R. Xiong, A.M. Grant, R. Ma, S. Zhang, V.V. Tsukruk, Naturally-derived biopolymer nanocomposites: interfacial design, properties and emerging applications, Mater. Sci. Eng. R. Rep. 125 (2018) 1–41.
[16] B.T. Mekonnen, M. Ragothaman, T. Palanisamy, Bifunctional hybrid composites from collagen biowastes for heterogeneous applications, ACS Omega 2 (2017) 5260–5270.
[17] Z. Tosun, P.S. McFetridge, A composite SWNT–collagen matrix: characterization and preliminary assessment as a conductive peripheral nerve regeneration matrix, J. Neural Eng. 7 (2010), 066002.
[18] C. Liu, X. Ye, X. Wang, X. Liao, X. Huang, B. Shi, Collagen fiber membrane as an absorptive substrate to coat with carbon nanotubes-encapsulated metal nanoparticles for lightweight, wearable, and absorption-dominated shielding membrane, Ind. Eng. Chem. Res. 56 (2017) 8553–8562.
[19] X. Wang, O. Yue, X. Liu, M. Hou, M. Zheng, A novel bio-inspired multi-functional collagen aggregate based flexible sensor with multi-layer and internal 3D network structure, Chem. Eng. J. 392 (2020), 123672.
[20] V. Vivekananthan, N.R. Alluri, Y. Purusothaman, A. Chandrasekhar, S. Selvarajan, S.-J. Kim, Biocompatible collagen nanofibrils: an approach for sustainable energy harvesting and battery-free humidity sensor applications, ACS Appl. Mater. Interfaces 10 (2018) 18650–18656.
[21] K. Yonathan, R. Mann, K.R. Mahbub, C. Gunawan, The impact of silver nanoparticles on microbial communities and antibiotic resistance determinants in the environment, Environ. Pollut. 293 (2022), 118506.
[22] J. Moreira, M.M. Fernandes, E.O. Carvalho, A. Nicolau, V. Lazic, J.M. Nedeljković, S. Lanceros-Mendez, Exploring electroactive microenvironments in polymer-based nanocomposites to sensitize bacterial cells to low-dose embedded silver nanoparticles, Acta Biomater. 139 (2022) 237–248.
[23] P.E. Antezana, S. Municoy, C.J. Pérez, M.F. Desimone, Collagen hydrogels loaded with silver nanoparticles and cannabis sativa oil. Antibiotics (Basel) (2021) 10.
[24] N. Duraipandy, R. Lakra, K. Vinjimur Srivatsan, U. Ramamoorthy, P.S. Korrapati, M.S. Kiran, Plumbagin caged silver nanoparticle stabilized collagen scaffold for wound dressing, J. Mater. Chem. B 3 (2015) 1415–1425.
[25] R. Khan, M.H. Khan, Use of collagen as a biomaterial: an update, J. Indian Soc. Periodontol. 17 (2013) 539–542.
[26] A. Wickham, M. Vagin, H. Khalaf, S. Bertazzo, P. Hodder, S. Dånmark, T. Bengtsson, J. Altimiras, D. Aili, Electroactive biomimetic collagen-silver nanowire composite scaffolds, Nanoscale 8 (2016) 14146–14155.

[27] L. Wang, P. Ni, G. Wei, J. Wang, Z. Li, Collagen nanofiber-templated silver nanowires on graphene nanosheets for a nonenzymatic amperometric biosensor of hydrogen peroxide, Chem. Lett. 43 (2014) 544–546.
[28] P. Zhang, I. Wyman, J. Hu, S. Lin, Z. Zhong, Y. Tu, Z. Huang, Y. Wei, Silver nanowires: synthesis technologies, growth mechanism and multifunctional applications, Mater. Sci. Eng. B 223 (2017) 1–23.
[29] K. Belbachir, R. Noreen, G. Goyspillou, C. Petibois, Collagen types analysis and differentiation by FTIR spectroscopy, Anal. Bioanal. Chem. 395 (2009) 829–837.
[30] T. Riaz, R. Zeeshan, F. Zarif, K. Ilyas, N. Muhammad, S.Z. Safi, A. Rahim, S.A. A. Rizvi, I.U. Rehman, FTIR analysis of natural and synthetic collagen, Appl. Spectroscopy Rev. 53 (2018) 703–746.
[31] M.G. Bridelli, Fourier transform infrared spectroscopy in the study of hydrated biological macromolecules. In: G. S. Nikolic, M.D. Cakic, D.J. Cvetkovic, (Eds.), Fourier Transforms - High-tech Application and Current Trends. IntechOpen, 2017.
[32] K. Krasniewska, S. Galus, M. Gniewosz, Biopolymers-based materilas containing silver nanoparticles as active packaging for food applications-a review, Int. J. Mol. Sci. 21 (2019) 698.
[33] S. Pandey, G.K. Goswami, K.K. Nanda, Green synthesis of biopolymer–silver nanoparticle nanocomposite: an optical sensor for ammonia detection, Int. J. Biol. Macromol. 51 (2012) 583–659.
[34] Y. Zhang, Z. Chen, X. Liu, J. Shi, H. Chen, Y. Gong, SEM, FTIR and DSC investigation of collagen hydrolysate treated degraded leather, J. Cult. Herit. 48 (2021) 205–210.
[35] M. Schroepfer, M. Meyer, DSC investigation of bovine hide collagen at varying degrees of crosslinking and humidifies, Int. J. Biol. Macromol. 103 (2017) 120–218.
[36] M.N. Taravel, A. Domard, Collagen and its interaction with chitosan: II. Influence of the physicochemical characteristics of collagen, Biomaterials 16 (1995) 865-71.
[37] A. Rochdi, L. Foucat, J.P. Renou, Effect of termal denaturation on water-collagen interactions: NMR relaxation and diferential scanning calorimetry analysis, Pept. Sci. 50 (1999) 690–696.
[38] V. Samouillan, F. Delaunay, J. Dandurand, N. Merbahi, J.-P. Gardou, M. Yousfi, A. Gandaglia, M. Spina, C. Lacabanne, The use of termal techniques for the characterization and selection for natural biomaterials, J. Funct. Biomater. 2 (2011) 230–248.
[39] R. Socrates, O. Prymak, K. Loza, N. Sakthivel, A. Rajaram, M. Epple, S. Narayana Kalkura, Biomimetic fabrication of mineralized composite films of nanosilver loaded native fibrillar collagen and chitosan, Mater. Sci. Eng. C 99 (2019) 357–366.
[40] W. Wang, X. Zhang, C. Li, G. Du, H. Zhang, Y. Ni, Using carboxylated cellulose nanofibers to enhance mechanical and barrier properties o collagen fiber film by electrostatic interaction, J. Sci. Food Agric. 98 (2017) 3089–3097.
[41] Z. Meng, X. Zheng, T. Tang, J. Liu, Z. Ma, Q. Zhao, Dissolution and regeneration of collagen fibers using ionic liquid, Int. J. Biol. Macromol. 51 (2012) 440–448.
[42] J. Cao, Q. Duan, X. Liu, X. Shen, C. Li, Extraction and physicochemical characterization of pepsin soluble collagens from golden pompano (Trachinotus blochii) skin and bone, J. Aquat. Food Prod. Technol. 28 (2019) 837–847.
[43] S. Thomas, N. Maiti, T. Mukherjee, S. Kapoor, Investigation on the absorption characteristics of anserine on the surface of colloidal silver nanoparticles. Spectrochimia Acta. Part A, Mol. Biomol. Spectroscopy. 112 (2013) 27-32.
[44] S.F. Mendes, C.M. Costa, C. Caparros, V. Sendacas, S. Lanceros-Méndez, Effect of filler size and concentration on the structure and properties of poly(vinylidene fluoride)/BaTiO3 nanocomposites, J. Mater. Sci. 47 (2012) 1378–1388.
[45] D. Corsino, M.D. Balela, Room temperature sintering of printer silver nanoparticle conductive ink, in: IOP Conference Series Materials Science and Engineering. 264, 012020, 2017.
[46] J.L. Zeng, Z. Cao, D.W. Yang, L.X. Sun, L. Zhang, Thermal conductivity enhancement of Ag nanowires on an organic phase change materials, J. Therm. Anal. Calorim. 101 (2010) 385–439.
[47] H. Wu, X. Huang, M.M. Gao, X.P. Liao, B. Shi, Polyphenol-grafted collagen fiber as reductant and stabilizer for one-step synthesis of size-controlled gold nanoparticles and their catalytic application to 4-nitrophenol reduction, Green Chem. 13 (2011) 651–658.
[48] M. Shu, F. He, Z. Li, X. Zhu, Y. Ma, Z. Zhou, F. Gao, M. Zeng, Biosynthesis and antibacterial activity of silver nanoparticles using yeast extract as reducing and capping agents, Nanoscale Res. Lett. 15 (2020) 14.
[49] M. Zienkiewicz-Strzałka, A. Deryło-Marczewska, Small AgNP in the biopolymer nanocomposite system, Int. J. Mol. Sci. 21 (2020) 9388.
[50] P. Kanmani, J.W. Rhim, Physicochemical properties of gelatin/silver nanoparticle antimicrobial composite films, Food Chem. 148 (2014) 162–169.
[51] F. Ortega, L. Giannuzzi, V.B. Arce, M.A. García, Active composite starch films containing green synthetized silver nanoparticles, Food Hydrocoll. 70 (2017) 152–162.
[52] S. Shankar, J.W. Rhim, Amino acid mediated synthesis of silver nanoparticles and preparation of antimicrobial agar/silver nanoparticles composite films, Carbohydr. Polym. 130 (2015) 353–363.
[53] G. Khanarian, J. Joo, X.-Q. Liu, P. Eastman, D. Werner, K. O'Connell, P. Trefonas, The optical and electrical properties of silver nanowire mesh films, J. Appl. Phys. 114 (2013), 024302.
[54] T.J. Silhavy, D. Kahne, S. Walker, The bacterial cell envelope. Cold Spring Harb Perspect Biol. 2,a000414-a, 2010.
[55] W.K. Jung, H.C. Koo, K.W. Kim, S. Shin, S.H. Kim, Y.H. Park, Antibacterial activity and mechanism of action of the silver ion in Staphylococcus aureus and Escherichia coli, Appl. Environ. Microbiol.. 74 (2008) 2171–2178.
[56] R.D. Turner, J.R. Wingham, T.E. Paterson, J. Shepherd, C. Majewski, Use of silver-based additives for the development of antibacterial functionality in Laser Sintered polyamide 12 parts, Sci. Rep. 10 (2020) 892.
[57] M. Andonegi, A. Irastorza, A. Izeta, S. Cabezudo, K. de la Caba, P. Guerrero, A green approach towards native collagen scaffolds: environmental and physicochemical assessment, Polymers 12 (2020) 1597.
[58] Q. Hua, J. Sun, H. Liu, R. Bao, R. Yu, J. Zhai, C. Pan, Z.L. Wang, Skin-inspired highly stretchable and conformable matrix networks for multifunctional sensing, Nat. Commun. 9 (2018) 244.
[59] N. Luo, J. Zhang, X. Ding, Z. Zhou, Q. Zhang, Y.-T. Zhang, S.-C. Chen, J.-L. Hu, N. Zhao, Textile-enabled highly reproducible flexible pressure sensors for cardiovascular monitoring, Adv. Mater. Technol. 3 (2018) 1700222.
[60] J.S. Lee, K.-Y. Shin, O.J. Cheong, J.H. Kim, J. Jang, Highly sensitive and multifunctional tactile sensor using free-standing ZnO/PVDF thin film with graphene electrodes for pressure and temperature monitoring, Sci. Rep. 5 (2015) 7887.
[61] S. Yu, X. Wang, H. Xiang, L. Zhu, M. Tebyetekerwa, M. Zhu, Superior piezoresistive strain sensing behaviors of carbon nanotubes in one-dimensional polymer fiber structure, Carbon 140 (2018) 1–9.
[62] S. Duan, Z. Wang, L. Zhang, J. Liu, C. Li, A Highly stretchable, sensitive, and transparent strain sensor based on binary hybrid network consisting of hierarchical multiscale metal nanowires, Adv. Mater. Technol. 3 (2018) 1800020.
[63] Y. Zhao, Y. Yang, L. Cui, F. Zheng, Q. Song, Electroactive Au@Ag nanoparticles driven electrochemical sensor for endogenous H2S detection, Biosens. Bioelectron. 117 (2018) 53–59.
[64] J. Ma, Z. Pan, W. Zhang, Q. Fan, W. Li, H. Liang, High-sensitivity microchannel-structured collagen fiber-based sensors with antibacterial and hydrophobic properties, ACS Sustain. Chem. Eng. 10 (2022) 16814–16824.
[65] W. Zhang, Z. Pan, J. Ma, L. Wei, Z. Chen, J. Wang, Degradable cross-linked collagen fiber/MXene composite aerogels as a high-performing sensitive pressure sensor, ACS Sustain. Chem. Eng. 10 (2022) 1408–1418.
[66] L. Ke, Y. Wang, X. Ye, W. Luo, X. Huang, B. Shi, Collagen-based breathable, humidity-ultrastable and degradable on-skin device, J. Mater. Chem. C 7 (2019) 2548–2556.